Molecular Biology of the Cell
Vol. 16, 1811–1822, April 2005

Mystique Is a New Insulin-like Growth Factor-I-regulated PDZ-LIM Domain Protein That Promotes Cell Attachment and Migration and Suppresses Anchorage-independent Growth[D]

Gary Loughran,* Nollaig C. Healy,* Patrick A. Kiely,* Merei Huigsloot,* Nancy L. Kedersha,† and Rosemary O'Connor*

*Cell Biology Laboratory, Department of Biochemistry, BioSciences Institute, National University of Ireland, Cork, Ireland; and †Division of Rheumatology and Immunology, Brigham and Women's Hospital, Boston, MA 02115

Submitted December 10, 2004; Accepted January 11, 2005
Monitoring Editor: Carl-Henrik Heldin

By comparing differential gene expression in the insulin-like growth factor (IGF)-IR null cell fibroblast cell line (R− cells) with cells overexpressing the IGF-IR (R+ cells), we identified the *Mystique* gene expressed as alternatively spliced variants. The human homologue of Mystique is located on chromosome 8p21.2 and encodes a PDZ LIM domain protein (PDLIM2). GFP-Mystique was colocalized at cytoskeleton focal contacts with α-actinin and β1-integrin. Only one isoform of endogenous human Mystique protein, Mystique 2, was detected in cell lines. Mystique 2 was more abundant in nontransformed MCF10A breast epithelial cells than in MCF-7 breast carcinoma cells and was induced by IGF-I and cell adhesion. Overexpression of Mystique 2 in MCF-7 cells suppressed colony formation in soft agarose and enhanced cell adhesion to collagen and fibronectin. Point mutation of either the PDZ or LIM domain was sufficient to reverse suppression of colony formation, but mutation of the PDZ domain alone was sufficient to abolish enhanced adhesion. Knockdown of Mystique 2 with small interfering RNA abrogated both adhesion and migration in MCF10A and MCF-7 cells. The data indicate that Mystique is an IGF-IR–regulated adapter protein located at the actin cytoskeleton that is necessary for the migratory capacity of epithelial cells.

INTRODUCTION

Insulin-like growth factor (IGF)-I and IGF-II are ligands for the widely expressed IGF-I receptor tyrosine kinase, which promotes mitogenesis and cell survival (reviewed in Adams *et al*., 2000). The IGF-IR is essential for normal growth during embryonic development and promotes cell survival and migration. Circulating IGFs and the IGF-IR signaling pathways also have been associated with cancer progression (reviewed in LeRoith and Roberts, 2003). In a mouse model of pancreatic islet cell tumorigenesis, endogenous IGF-IR expression was up-regulated at invasive regions of the tumors, and ectopic IGF-IR expression resulted in the accelerated development of highly invasive and metastatic carcinomas (Lopez and Hanahan, 2002). Conversely, the suppression of IGF-IR expression by antisense strategies (Resnicoff, 1998) or blocking antibodies results in decreased tumor growth and decreased metastatic capacity in tumor cell models (Maloney *et al*., 2003). Signals from the IGF-IR associated with survival, tumorigenicity, and metastasis are associated with the C terminus of the receptor (O'Connor *et al*., 1997; Brodt *et al*., 2001; Baserga *et al*., 2003).

This article was published online ahead of print in *MBC in Press* (http://www.molbiolcell.org/cgi/doi/10.1091/mbc.E04–12–1052) on January 19, 2005.

[D] The online version of this article contains supplemental material at *MBC Online* (http://www.molbiolcell.org).

Address correspondence to: Rosemary O'Connor (r.oconnor@ucc.ie).

Cell migration and invasion are complex processes that require the coordination of signals from both adhesion and growth factor receptors. Signals from the IGF-IR can interact with those from integrins to initiate the formation of signaling complexes necessary for the formation and disassembly of cell adhesions with the extracellular matrix (ECM) (Doerr and Jones, 1996; Brooks *et al*., 1997). These signals involve enhancement of Shc phosphorylation (Mauro *et al*., 1999; Jackson *et al*., 2000; Kim *et al*., 2004), regulation of focal adhesion kinase phosphorylation at focal adhesions (Manes *et al*., 1999), differential regulation of signals by scaffolding proteins such as RACK1 (Hermanto *et al*., 2002; Kiely *et al*., 2002), signals from reorganization of the cytoskeleton (Casamassima and Rozengurt, 1998; Kim and Feldman, 1998; Guvakova *et al*., 2002), expression of angiogenic and invasive factors (Zhang *et al*., 2003), regulation of cadherin location (Playford *et al*., 2000; Pennisi *et al*., 2002), and transactivation of the epidermal growth factor (EGF) receptor (Burgaud and Baserga, 1996; Roudabush *et al*., 2000). How all of these events are coordinated during cell migration or invasion, or how some of these signals are enhanced in metastatic cancer, is still poorly understood.

IGF-I induces expression of several genes that promote cell migration and cancer progression, including β-catenin (Playford *et al*., 2000), the cadherin complex protein ZO-1 (Mauro *et al*., 2001), the angiogenic factor vascular endothelial growth factor (Miele *et al*., 2000), the metalloprotease MT1 MMP (Zhang and Brodt, 2003), and heparin-binding EGF-like growth factor (Mulligan *et al*., 2002). Mouse embryonic fibroblasts derived from the IGF-IR knockout mouse (R− cells) do not form colonies in soft agarose and are

refractory to cellular transformation by several oncogenes (Sell *et al*., 1994), but reexpression of the *Igf1r* gene in R− cells (the R+ cell line) restored the ability to become transformed (Sell *et al*., 1994). Thus, we hypothesized that R+ cells would express genes that are important for IGF-IR–mediated cell growth or migration at higher levels than R− cells.

To identify such genes, we used a combination of suppressive subtractive hybridization (SSH) and cDNA arrays. From this, we isolated the *Mystique* gene, which encodes a PDZ-LIM protein that is also called PDLIM2 in the human genome. Mystique is the newest member of the alkaline phosphatase (ALP) (Pomiáes *et al*., 1999), RIL (Bashirova *et al*., 1998), and CLP-36 (Wang *et al*., 1995) subfamily of PDZ-LIM domain proteins.

PDZ domains are 80- to 100-amino acid domains that mediate specific protein–protein interactions and have an essential role in the assembly of protein complexes (Ponting *et al*., 1997; Huang *et al*., 2003). LIM domains are cysteine-rich zinc finger motifs (Michelsen *et al*., 1993; Ponting *et al*., 1997) that serve as protein binding interfaces (Schmeichel and Beckerle, 1994) and are found in transcription factors, kinases, and in scaffolding proteins such as zyxin and paxillin (reviewed in Bach, 2000). Proteins containing LIM domains have essential roles in cell fate decisions during development, in cytoskeletal organization, and also have been associated with oncogenesis (reviewed in Bach, 2000).

In this study, we determined that Mystique is localized at the actin cytoskeleton and its expression is regulated by IGF-I and adhesion in both MCF-7 breast carcinoma and MCF10A nontransformed epithelial cells. Overexpression of Mystique in MCF-7 cells suppressed anchorage-independent growth as colonies in soft agarose but enhanced cell attachment to ECM proteins. A point mutation in the PDZ domain abolished promotion of attachment and association with α-actinin, whereas mutation of either the PDZ or LIM domain abolished the effect on suppression of clonogenic growth. Silencing of Mystique expression with siRNA resulted in impaired attachment and migration in MCF-7 and MCF10A cells. Together, the data suggest that Mystique acts at the actin cytoskeleton in epithelial cells to promote interactions with ECM proteins that are essential for cell migration.

MATERIALS AND METHODS

Cell Culture and Transfection

R− cells are an embryonic fibroblast cell line derived from mice with a targeted disruption of the IGF-IR, and R+ cells are R− cells that were transfected to express the IGF-IR (Sell *et al*., 1994). R+, R−, HeLa, and MCF-7 cell lines were maintained in DMEM (BioWhittaker UK, Berkshire, United Kingdom) supplemented with 1 mM L-glutamine, 10% fetal bovine serum (FBS), and antibiotics. MCF10A cells were maintained in DMEM/Ham's medium (Sigma Ireland, Dublin, Ireland) supplemented with 5% horse serum, 1 μg/ml insulin, 20 ng/ml EGF (PeproTech, London, United Kingdom), 100 ng/ml cholera toxin, 0.5 μg/ml hydrocortisone, and 2 mM L-glutamine. For IGF-I stimulations, MCF-7 and MCF10A cells were starved of serum for 24 h before the addition of 100 ng/ml IGF-I (PeproTech) for the indicated times. For culturing cells in suspension, 2×10^6 cells were seeded onto nontissue culture plates that had been coated with poly-HEMA (6 mg/ml) (Sigma Ireland).

For transient transfections of HeLa cells with green fluorescent protein (GFP)- or hemagglutinin (HA)-tagged Mystique isoforms, cells were transfected with 4 μg of DNA by using LipofectAMINE Plus (Invitrogen, Breda, The Netherlands). To generate stable transfectants, MCF-7 cells were transfected with relevant plasmids, and 24 h after transfection cells were cultured in medium containing G418 (Geneticin; 1 mg/ml) for 14 d, at which time individual clones were selected, expanded, and screened for expression of HA-Mystique isoforms by Western blotting.

Northern Blotting

RNA from 5×10^6 cells was extracted using the TRIzol reagent (Invitrogen) according to the manufacturer's instructions and separated by denaturing formaldehyde gel electrophoresis and transferred to nylon membranes. Prehybridization and hybridization were carried out at 42°C in 50% formamide, 5× SSC, 4× Denhardt's solution, 0.1% SDS, and salmon sperm DNA (100 μl/ml; Sigma Ireland) for 2 and 15 h, respectively. ^{32}P-Labeled probes (>1×10^6 cpm/ml) were prepared by the random primer method (NEBlot, New England Biolabs, Hertfordshire, United Kingdom). Filters were washed twice at 42°C in 2× SSC, 0.1% SDS for 5 min., and then twice at 42°C in 0.1× SSC, 0.1% SDS for 15 min, and exposed to PhosphorImager screens for empirically determined times.

Molecular Cloning of Mystique

Mystique 2 was amplified by reverse transcription-polymerase chain reaction (RT-PCR) on total RNA extracted from MCF-7 cells by using the following primers: MF 5′-ctt**ctcgag**gtatggcgttgacgg-3′ and M2R 5′-cat**ctcgag**ctcaggccgagag-3′. Two distinct products of ~1.0 and ~0.9 kb were amplified, purified, and cloned using *Xho*I (bold sequences in primers) into pcDNA3-HaX and pEGFP-C1 (BD Biosciences, Oxford, United Kingdom). Sequencing of inserts confirmed the larger insert (1.0 kb) to be *Mystique 2* and the smaller insert (0.9 kb) to be two splice variants of the same size, which we designated *Mystique 3a* and *Mystique 4* (see Supplemental Figures 1 and 2). *Mystique 1* was cloned after polymerase chain reaction (PCR) amplification with primers MF (as described above) and M1F 5′-aga**ctcgag**cacaccagcttggc-3′ on human cDNA clone FLJ00106 (kindly provided by the Kazusa DNA Research Institute, Chiba, Japan). *Mystique 2* L80K, CC313-316, and double mutants were generated by PCR by using the *Pvu*II (L80K) and *Kpn*I (CC313-316SS) restriction sites within *Mystique 2* and then cloned *Xho*I/*Xho*I into pcDNA3-HaX and pEGFP-C1 vectors.

Mystique Antiserum

A Mystique restriction fragment encoding amino acids 1–184 (including the PDZ domain) was cloned into pGEX-6P1 prokaryotic expression vector (Pfizer, Inc., Täby, Sweden). Glutathione *S*-transferase (GST)-fused 1–184 protein was purified by affinity chromatography and injected into a New Zealand White rabbit (Biological Services Unit, UCC, Cork, Ireland). Affinity-purified polyclonal antibodies were obtained by adsorption to nitrocellulose-immobilized GST-fused 1–184 fragment, elution with 500 μl of 0.2 M glycine, pH 2.15, neutralization with 200 μl of 1 M K_2HPO_4, pH 7.0, and extensive dialysis against 1× phosphate-buffered saline at 4°C.

Antibodies and Immunofluorescence

Mouse anti-paxillin and anti-phosphotyrosine antibodies were purchased from Upstate Biotechnology (Milton Keynes, United Kingdom). Mouse anti-α-actinin (clone BM75.2) and anti-β-actin antibodies were from Sigma-Ireland. Mouse anti-β1-integrin (clone 12G10) was from Serotec (Oxford, United Kingdom). Mouse anti-HA (clone 16B12) was from Babco (Berkeley, CA).

For immunofluorescence, glass coverslips were coated with 10 μg/ml collagen I (Sigma Ireland) at 4°C overnight. Cells were then allowed to attach onto precoated coverslips for at least 12 h, rinsed with PHEM (60 mM PIPES, 25 mM HEPES, 10 mM EGTA, and 2 mM $MgCl_2$, pH 6.9), fixed in 3.7% formaldehyde in PHEM for 10 min, and permeabilized with 0.1% Triton X (TX)-100 in PHEM for 5 min. After preblocking with 5% normal goat serum (Sigma Ireland) in PHEM for 30 min, cells were incubated with primary antibody, washed with PHEM, and incubated with Cy2- or Cy3-conjugated secondary antibody (Jackson ImmunoResearch Laboratories, Soham, Cambridgeshire, United Kingdom). For the detection of F-actin, cells were treated with tetramethylrhodamine B isothiocyanate (TRITC)-phalloidin (Sigma Ireland).

Fluorescence was monitored using a 100× Plan Fluor objective on a Nikon Eclipse E600 microscope. Images were taken with a SPOT camera and adjusted using Adobe Photoshop or MetaMorph software.

Western Blotting and Immunoprecipitation

Whole cell lysates were prepared by lysing cells in ice-cold SDS-lysis buffer (1% Nonidet P-40, 0.1% SDS, 20 mM Tris, 50 mM NaCl, 50 mM sodium fluoride, 1 μM pepstatin, 1 mM phenylmethylsulfonyl fluoride, 1 μM aprotinin, and 1 mM sodium orthovanadate, pH 7.6). Cell debris was removed by centrifugation at 15,000 × *g* at 4°C for 15 min, and samples were then denatured by boiling in 5× SDS-PAGE sample buffer for 5 min. Detergent-soluble fractions were prepared by lysing cells in ice-cold CSK extraction buffer (10 mM PIPES, pH 6.8, 100 mM NaCl, 300 mM sucrose, 3 mM $MgCl_2$, and 1 mM EGTA) with 0.5% TX-100 and protease inhibitors. Detergent-insoluble material was pelleted by centrifugation and pellets were resuspended in 2% SDS, 50 mM Tris, pH 7.5.

Proteins were resolved using 4–20% gradient SDS-PAGE and transferred to nitrocellulose membranes (Schleicher & Schuell, Dublin, Ireland), which were blocked with 5% milk in Tris-buffered saline (TBS)-T (20 mM Tris, 150 mM NaCl, and 0.05% Tween 20, pH 7.6) for 1 h at room temperature. Antibodies were diluted in TBS-T, 5% milk and incubated at 4°C overnight. Horseradish

peroxidase-conjugated secondary antibodies (DakoCytomation Denmark A/S, Glostrup, Denmark) were used for detection using chemiluminescence with the enhanced chemiluminescence reagent (Amersham Biosciences UK, Little Chalfont, Buckinghamshire, United Kingdom).

For immunoprecipitation of endogenous α-actinin or transfected HA-tagged Mystique 2 mutants, protein extracts were precleared using bovine serum albumin (BSA)-coated protein G Agarose beads (15 μl of beads per 400 μg of total protein in 700 μl of lysis buffer) by incubation at 4°C for 1 h with gentle rocking. The lysates were recovered from the beads by centrifugation at 1000 × *g* for 3 min and transferred to fresh tubes for incubation with 20 μl of protein G Agarose beads plus primary antibody (3 μg of each antibody) overnight at 4°C with gentle rocking. The beads were washed (3 times) with ice-cold lysis buffer and then removed from the beads by boiling for 5 min in 20 μl of 2× SDS-PAGE sample buffer for electrophoresis and Western blot analysis.

Proliferation and Soft Agar Assays

To measure proliferation in monolayer culture, MCF-7 stable transfectants were cultured in DMEM/10% FBS at 4×10^4 cells per well in multiple wells of a 24-well plate. At intervals, cells were removed from quadruplicate wells and counted by trypan blue exclusion using a hemocytometer.

Anchorage-independent growth was determined by assaying colony formation in soft agarose. MCF-7 cells (10^3/well) were resuspended in 0.33% low-melting point agarose (Sigma Ireland) in DMEM/10% FBS and plated in triplicate onto 35-mm dishes containing a 2-ml base agarose layer (0.5%). Every 3–4 d, 200 μl of DMEM/10% FBS was added. After 14 d, colonies were stained with 0.01% crystal violet.

Adhesion Assays

Plates (96-well) were coated with either collagen I (10 μg/ml) or fibronectin (5 μg/ml) at 4°C overnight and then blocked with 2.5% BSA for 2 h at 37°C. Cells were starved from serum for 4 h before harvesting with trypsin/EDTA, washing twice with serum-free media (SFM) and then resuspending in SFM 0.01% BSA (DMEM/BSA). The final cell number was determined, and 2×10^4 cells per well were resuspended in DMEM/BSA and plated onto collagen I- or fibronectin-coated plates. Cells were allowed to attach at 37°C for the times indicated, and unbound cells were removed by gentle washing with DMEM/BSA. Attached cells were then fixed with methanol and stained with 0.1% crystal violet, which was extracted after extensive washing with 50 μl of 0.5% TX-100 (in water) at room temperature. Incorporated crystal violet was measured by reading its absorbance at A_{595}.

Small Interfering RNA (siRNA) Construction and Transfection

siRNAs targeted to human and mouse *Mystique* were obtained from Dharmacon (Lafayette, CO) with the following sequences: human *Mystique*, 5′-aagauccgccagagccccucg-3′; and mouse *Mystique*, 5′-aagauccg**a**cagagc**g**cucu**a**-3′ (corresponding to nucleotides 199–219 after the start codon for both human and mouse *Mystique*). Nucleotides typed in bold indicate where the mouse siRNA differs from the human. MCF-7 and MCF10A cells (30–50% confluent) were transfected with 20 pmol of siRNA by using the OligofectAMINE transfection reagent (Invitrogen) according to the manufacturer's instructions. Protein expression was assessed by Western blotting with the anti-Mystique antiserum from 48 to 96 h after transfection. Adhesion and transwell migration assays were performed 60 h posttransfection.

Transwell Migration Assays

siRNA-transfected MCF-7 and MCF10A cells were starved of serum for 4 h before harvesting with trypsin/EDTA, washing twice with SFM, and then resuspending in DMEM/BSA. The final cell density was determined using a hemocytometer, and 2.5×10^4 cells were resuspended in 100 μl of DMEM/BSA. Lower wells were loaded with either DMEM/bovine serum albumin (control) or DMEM/BSA 10% FBS. After 4 h (MCF10A) or 18 h (MCF-7) at 37°C, chambers were disassembled and cells on the upper surface of the membrane were removed by scraping so that only cells that had migrated through the membrane remained. The membrane was then fixed with methanol, stained with 0.1% crystal violet, washed extensively with water, and air-dried. Cell counts were obtained by averaging cells from five fields at 10× magnification per well from triplicate wells.

RESULTS

Mystique Encodes Proteins with Homology to an Emerging Family of PDZ-LIM Domain Proteins

To identify genes that encode potential regulators of IGF-IR–mediated transformation, we used SSH in combination with cDNA arrays to compare gene expression between R− (Sell *et al*., 1994) and R+ cells. From this screen, we identified a partial cDNA (446 base pairs) with sequence identity to the 3′-untranslated region (UTR) (base pairs 1055–1501) of a previously uncharacterized mouse cDNA, *Mystique* (PDLIM2; accession no. BC024556). This *Mystique* cDNA clone was obtained from the IMAGE consortium and used to probe Northern blots generated from R+ and R− cells. *Mystique* hybridized with at least three RNA species in R+ and R− cells (Figure 1A). Two transcripts (~4.3 kb [top arrow] and ~1.8 kb [middle arrow]) were more abundant in R+ cell RNA, whereas one transcript (~1.5 kb [bottom arrow]) was more abundant in R− cell RNA. The predicted size of the R− cell-enriched transcript (~1.5 kb, bottom arrow; Figure 1A) matched the size of *Mystique* cDNA (1.55 kb; BC024556). However, BC024556 may not be the full-length cDNA. Other than expressed sequence tags, only one mouse *Mystique* cDNA sequence has been entered into the public databases (BC024556). Therefore, we investigated human *Mystique* cDNAs.

In humans, three *Mystique* cDNAs have undergone preliminary National Center for Biotechnology Information validation: *Mystique 1* (~4.6 kb), *Mystique 2* (~1.85 kb), and *Mystique 3* (~1.5 kb). The sizes of these three human cDNAs closely match the predicted sizes of the three mouse transcripts that hybridized with mouse *Mystique* on Northern blots (Figure 1A). Alignment of the three *hMystique* variants to the human genome indicates that they are splice variants of a single gene (~20 kb) located on human chromosome 8p21.2. (Supplemental Figure 1).

Alignment of mouse *Mystique* with human *Mystique* cDNAs indicates that mouse *Mystique* (1.55 kb; BC024556) is homologous to *Mystique 2* (1.85 kb; 77% identity at amino acid level) and that the mouse homologue is missing ~300 base pairs of 5′-UTR, which accounts for the difference in size between these two cDNAs. Therefore, it is likely that, in mouse, the 4.5-kb upper transcript in Figure 1A is mouse *Mystique 1*, the 1.8-kb middle transcript is *Mystique 2*, and the lower 1.5-kb transcript is *Mystique 3*.

To investigate *Mystique* expression in different organs, a murine multiple tissue Northern blot (Figure 1B) was probed with *Mystique*. *Mystique 2* is the predominant mRNA in most tissues with high expression in lung; moderate expression in kidney, testis, and spleen; and low expression in heart and brain. Only in heart and brain is *Mystique 3* RNA more abundant than *Mystique 2*. Interestingly, unlike CLP-36 and ALP, *Mystique* is not expressed in skeletal muscle.

Human *Mystique 1*, *2*, and *3* are predicted to encode three different protein products: Mystique 1 (39.2 kDa), 2 (37.5 kDa), and 3 (29.1 kDa), respectively (Figure 1C and Supplemental Figure 2). *Mystique 1* and *2* are both predicted to code for proteins with one N-terminal PDZ domain and a single C-terminal LIM domain, with Mystique 1 differing from Mystique 2 only in the residues C-terminal to the LIM domain (Supplemental Figure 1). The absence of exon 9 from *Mystique 3* results in premature termination and is predicted to encode a PDZ-only protein (Supplemental Figure 1).

Mystique 2 shares homology to a recently characterized subfamily of cytoskeletal-associated PDZ-LIM domain proteins that includes CLP-36 (Wang *et al*., 1995), ALP (Pomiáes *et al*., 1999), and RIL (Bashirova *et al*., 1998). All four family members have similar structure with an N-terminal PDZ domain separated from a single C-terminal LIM domain by ~200 amino acids. Homology between these proteins is most conserved in the PDZ (48%) and LIM (54%) domains (Figure 1D).

We concluded that both the 4.5- and 1.8-kb transcripts that are abundant in R+ cell RNA code for Mystique 1 and

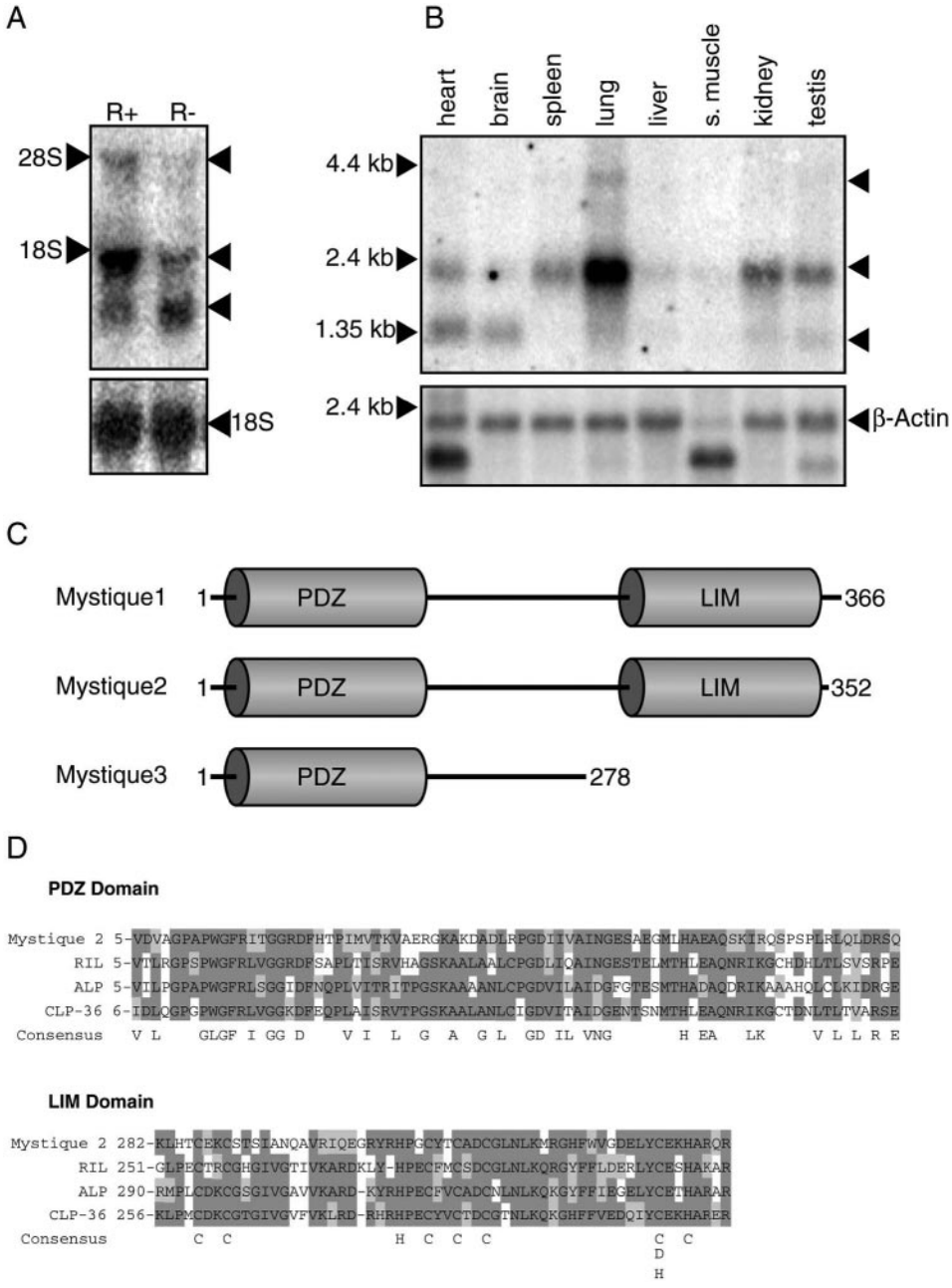

Figure 1. Mystique is expressed as at least three variants and encodes a protein with homology to an emerging family of PDZ-LIM domain proteins. (A) A Northern blot of R+ and R− cell RNA was probed with mouse Mystique cDNA followed by a probe to detect 18S RNA as a loading control. (B) A murine multiple tissue Northern blot was probed with mouse Mystique and β-actin cDNA probes. (C) The PDZ and LIM domains in human Mystique isoforms are illustrated. (D) Mystique PDZ and LIM domains were aligned with those of RIL, ALP, and CLP-36. Identical amino acids are shaded dark gray and similar amino acids are shaded in light gray.

Mystique 2, respectively. Both of these proteins have PDZ and LIM domains. However, Mystique 3, which is more abundant in R− cells, encodes a PDZ only protein.

Mystique Isoforms Associate with the Cytoskeleton

To investigate the subcellular location of Mystique, GFP- and HA-tagged expression constructs of the human Mystique, variants were generated using cDNAs derived by RT-PCR from MCF-7 cells (see *Materials and Methods* and supplemental data for description of Mystique variants). Transient expression of GFP-Mystique 1, 2, and 3a into HeLa cells demonstrated that Mystique 1 and 2 were predominantly localized at the cytoskeleton (Figure 2A). In contrast, Mystique 3a was seen predominantly in the nucleus and only seen slightly at the cytoskeleton (Figure 2A). Similar patterns of staining were evident in cells transfected with HA-tagged Mystique isoforms (our unpublished data).

Overexpression of HA-tagged Mystique isoforms 1, 2, and 3a in COS cells indicated that isoforms 1 and 3a were predominantly found in the TX-100–insoluble fraction (cytoskeleton and nucleus), whereas Mystique 2 was equally distributed between the detergent-soluble and -insoluble fraction (Figure 2B).

To detect endogenous Mystique isoforms, a rabbit antiserum was raised against the human PDZ domain, which is present in Mystique 1, 2, and 3a. In Western blot analysis of cell lysates from R+ and R− cells, a major immunoreactive band at ~38 kDa was more abundant in R+ cells compared with R− cells (Figure 2C). This band corresponds to the predicted size of Mystique 1 (39.2 kDa) and/or Mystique 2

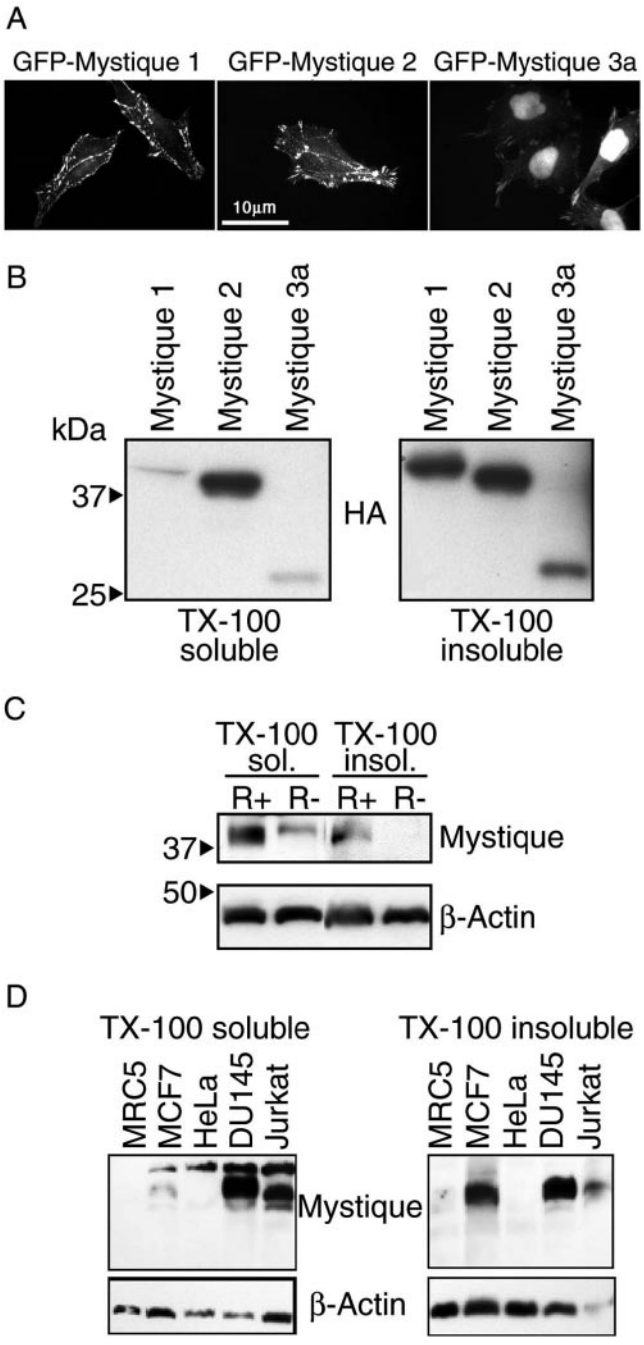

Figure 2. Mystique is a cytoskeleton-associated protein. (A) HeLa cells were transiently transfected with GFP-tagged Mystique 1, 2, or 3a and examined by fluorescence microscopy. (B) COS cells were transiently transfected with HA-tagged Mystique isoforms and TX-100–soluble proteins were extracted from cells (left) and TX-100–insoluble proteins (right) for Western blotting with anti-HA antibody. (C) Western blots were prepared with TX-100–soluble and –insoluble protein fractions extracted from R+ and R− cells and probed with anti-Mystique antiserum or anti-β-actin antibody. (D) Western blots prepared with TX-100–soluble and –insoluble protein extracts from MRC-5, MCF-7, HeLa, DU145, and Jurkat cells were probed with anti-Mystique antiserum and with anti-β-actin antibody.

(37.5 kDa), and this pattern of protein expression matches the pattern of *Mystique 1* and/or *Mystique 2* mRNA expression pattern observed in R+ and R− cells (Figure 1A). There was no band of the predicted size of Mystique 3 (27 kDa) detected in either R+ or R− cells (our unpublished data). Mystique 2 could not be detected in the TX-100–insoluble fraction of R− cells but again was similarly distributed in the TX-100–soluble and –insoluble fractions of R+ cells (Figure 2C). Mystique 2 also was detected in MCF-7 cells at low levels, in DU145 cells and Jurkat cells at higher levels, but not in HeLa cells or the fibroblast cell line MRC5 (Figure 2D).

Overall, the data indicate that Mystique 2 is the only isoform of the protein detectable in cells, and because Mystique 2 was found in both the TX-insoluble and -soluble fractions of all the cell lines except R−, MRC-5, and HeLa cells, it may translocate between the cytoskeleton and cytoplasm.

Mystique 2 Colocalizes with β1-Integrins and α-Actinin but Not with Paxillin or Phosphotyrosine

Mystique 2 is the only endogenous isoform detectable in cells, so we focused our attention on characterization of this protein. We first asked what other proteins it may colocalize with in cells. CLP-36, RIL, and ALP have previously been shown to associate with the actin cytoskeleton via the actin cross-linking protein α-actinin (Pomiáes *et al*., 1999; Zhou *et al*., 1999; Kotaka *et al*., 2000). Immunofluorescence with anti-Mystique antiserum on MCF-7 cells transiently overexpressing Mystique 2 indicated that Mystique 2 colocalizes with α-actinin (Figure 3). However, colocalization of Mystique 2 with paxillin or with phosphotyrosine staining was not evident, whereas substantial colocalization with β1-integrin was evident (Figure 3). This suggests that Mystique is located at the points of focal contacts toward the end of stress fibers, where α-actinin has previously been demonstrated to colocalize with β1-integrins but not with paxillin and phosphotyrosine (Rottner *et al*., 2001).

Overexpression of Mystique 2 Suppresses Anchorage-independent Growth, and This Function Requires Both the PDZ and LIM Domains

We next investigated the functions of Mystique in the monolayer and anchorage-independent growth of transformed cells. To determine the relative contributions of the Mystique 2 PDZ and LIM domains, we generated a series of Mystique 2 point mutants. A critical leucine residue in the PDZ domain (L80) was mutated to lysine (L80K) (Shieh and Niemeyer, 1995) and the second Zn-binding site of the LIM domain (Michelsen *et al*., 1993) was mutated by replacing two critical cysteines with serines (CC313-316SS). In addition, a double mutant containing both L80K and CC313-316SS mutations was generated (Figure 4A).

Three MCF-7 cell clones that overexpressed either HA-tagged-Mystique 2 (WT), Mystique 2 L80K (L80K), Mystique 2 CC313-316SS (CC-SS), Mystique 2 L80K-CC313–316SS (Double), or empty vector control (Neo) were isolated and the expression levels of Mystique 2 are shown in Figure 4B.

Three Neo and three WT clones where compared for monolayer (anchorage-dependent) growth, and results shown in Figure 4C indicated little difference in proliferation over 7 d. However, when Neo and WT clones were tested for their ability to form colonies in soft agarose (anchorage-independent growth), a dramatic decrease in colony number was observed in cells overexpressing WT Mystique 2 (Figure 4D). In contrast, cells expressing the L80K, CC-SS, or double mutant had comparable numbers of colonies to Neo cells.

Together, the data indicate that overexpression of Mystique 2 suppresses anchorage-independent growth of MCF-7 cells and that this suppression of clonogenic growth can be reversed by mutation of either the PDZ or LIM domain.

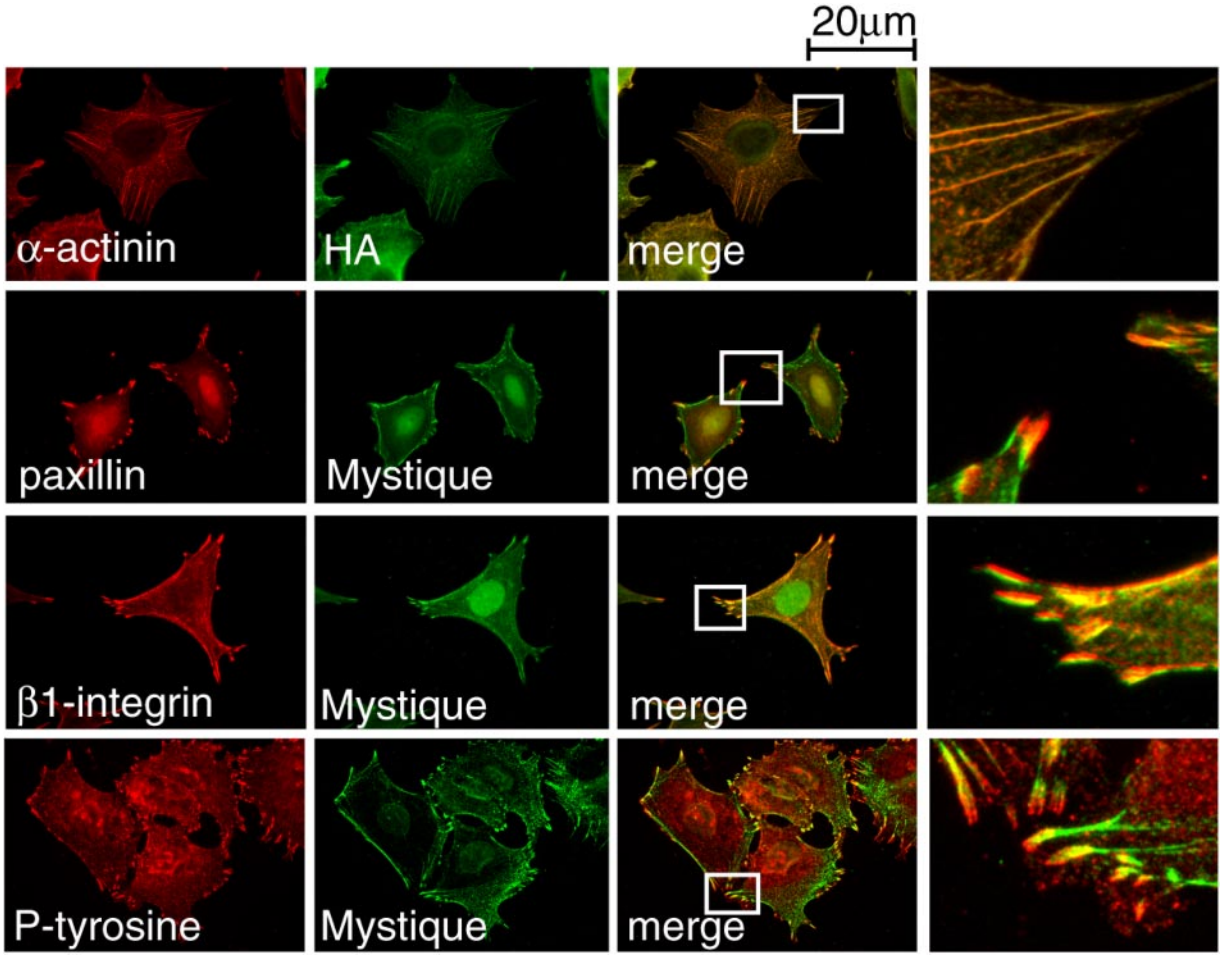

Figure 3. Localization of HA-Mystique 2 relative to α-actinin, paxillin, β1-integrin, and phosphotyrosine in MCF-7 cells. MCF-7 cells transiently expressing HA-tagged Mystique 2 were grown on collagen-coated coverslips. Cells were fixed and stained with either anti-HA antibody or anti-Mystique antiserum as indicated, which was detected by Cy2-labeled secondary antibody (green). Cells also were stained with either α-actinin, paxillin, β1-integrin, or phosphotyrosine antibodies as indicated, which were detected with Cy3-labeled secondary antibody (red). Amplified areas from the merged images are shown in the far-right panels.

Mystique 2 Expression Is Regulated by Adhesion in Transformed and Nontransformed Cells

The data with overexpressed Mystique 2 suggest it possesses tumor suppressor function, which seems inconsistent with it being a gene more highly expressed in transformed R+ cells than in nontransformed R− cells. We therefore investigated Mystique 2 expression in the nontumorigenic breast epithelial cell line MCF10A compared with MCF-7 cells and R+ cells. This demonstrated that Mystique 2 expression was ~10-fold higher in MCF10A cells than in MCF-7 cells or in R+ cells (Figure 5A). In addition, Mystique 2 expression was decreased in both MCF-7 and MCF10A cells upon serum starvation, but it could be induced after 1 h of IGF-I stimulation (Figure 5B).

Because Mystique 2 inhibition of MCF-7 cell clonogenic growth was achieved when Mystique 2 expression was under the control of an ectopic constitutively active promoter, we next asked whether endogenous levels of Mystique 2 change under anchorage-independent conditions. R+ cells, MCF-7 cells, and MCF10A cells were detached and held under anchorage-independent conditions by plating cells onto poly-HEMA–coated plates before analysis of endogenous Mystique 2 expression. Figure 5C demonstrates that Mystique 2 expression was greatly reduced when cells were cultured on poly-HEMA–coated plates. Furthermore, Mystique 2 levels increased when cells were allowed to reattach to tissue culture plates. This suggests that Mystique 2 is normally expressed and functions only when cells are attached to a substratum. The data also suggest that Mystique 2 expression may be quenched when cells acquire the ability to grow in anchorage-independent conditions or become transformed.

Overexpression of Mystique 2 Enhances Attachment to Collagen and Fibronectin and This Requires an Intact PDZ Domain

Because Mystique 2 is located at the cytoskeleton and is regulated by cell adhesion, we next investigated the effect of Mystique 2 overexpression on cell attachment to ECM proteins and cell migration. MCF-7 clones overexpressing wild-type Mystique 2 were compared with Neo control cells by allowing cells to adhere to either collagen or fibronectin. Overexpression of Mystique 2 caused a significant increase in adhesion to both collagen and fibronectin that was already evident after just 15 min (Figure 6A). Similar experiments with MCF-7 cells expressing Mystique 2 mutants

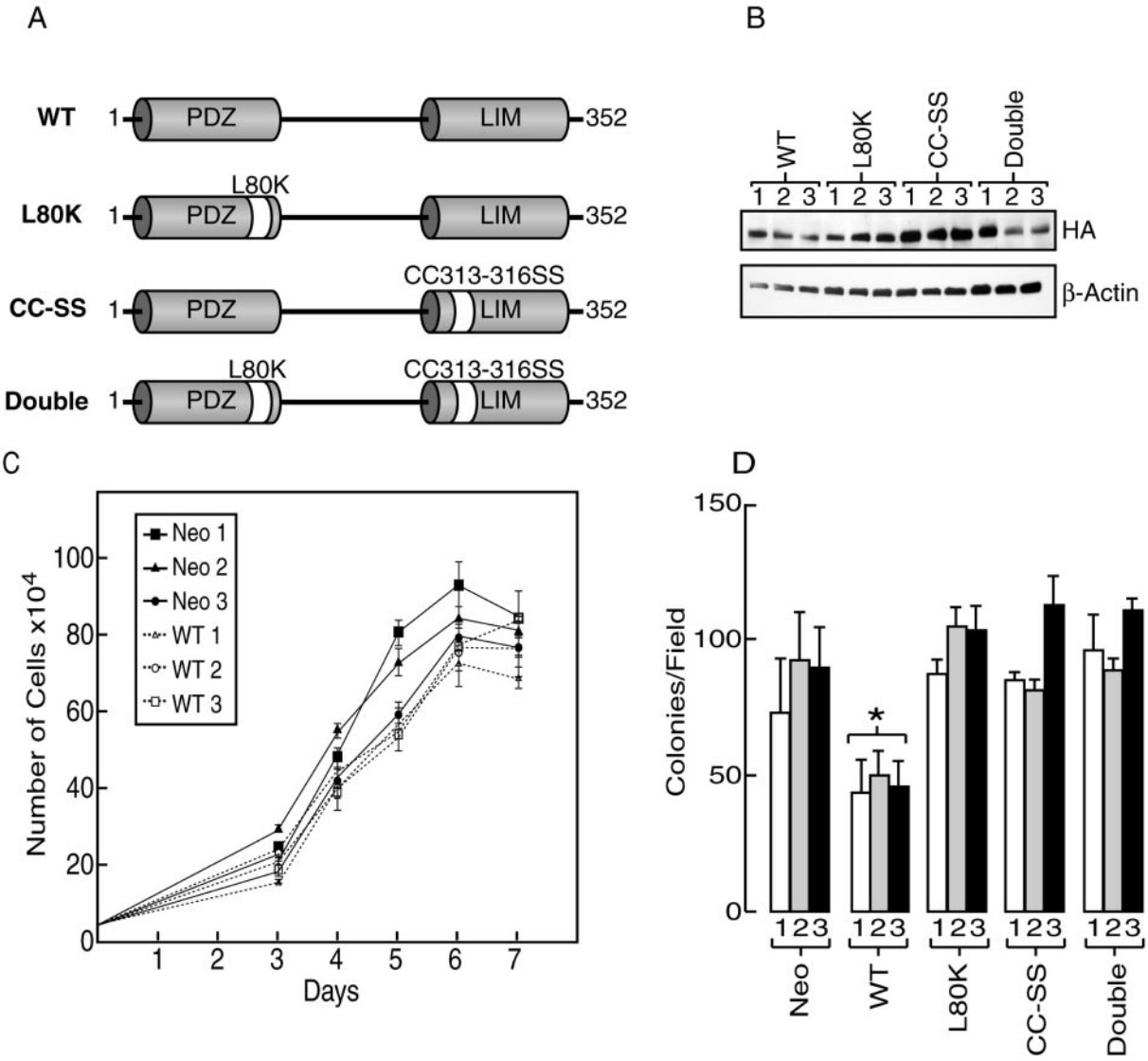

Figure 4. Stable overexpression of Mystique 2 inhibits anchorage-independent cell growth. (A) Point mutations of HA-Mystique 2 were generated as outlined in *Materials and Methods*. The amino acid positions of the mutations in the PDZ (L80K) and LIM (CC313–316SS) domains are illustrated. (B) Three MCF-7 cell clones that stably expressed either WT or the different Mystique 2 mutants were isolated and tested for expression of HA-Mystique by Western blotting with the anti-HA antibody. (C) MCF-7 clones were assessed for proliferation rates in monolayer culture >7 d. Wild-type Mystique 2-overexpressing cells (broken lines) were compared with Neo control cells (solid lines). Data are presented as the mean and SD of counts from quadruplicate wells and represent one of at least three independent experiments with similar results. (D) Mystique 2 WT and mutant-overexpressing MCF-7 clones were compared with Neo control clones for clonogenic growth in soft agarose. Each clone was plated in triplicate wells, and after 10 d the number of colonies from five fields per well was counted. The mean number of colonies per field for each well of each clone was averaged for each transfected construct (i.e., the means of WT clones 1–3 were averaged) and compared with the means of Neo clones 1–3 by using the Students *t*-test (*$p < 0.01$).

(Figure 6B) indicated that the CC-SS (LIM domain) mutant enhanced cell attachment, albeit slightly less than WT. However, the L80K (PDZ domain) mutant not only reversed the enhanced adhesion observed with WT but also exhibited less cell adhesion than Neo control cells. This suggests that the PDZ mutant suppresses endogenous Mystique 2 function, which is indicative of dominant negative function.

We also investigated the migratory capacity of MCF-7 cells overexpressing either WT or mutant Mystique 2 proteins in Transwell assays. This revealed no significant differences in cell migration for the clones described in Figures 4–6. However, WT clones that overexpressed the protein at high levels demonstrated enhanced migration (our unpublished data).

The PDZ domain of RIL, CLP-36, and ALP plays a central role in targeting these proteins to the cytoskeleton via its interactions with the actin cross-linking protein α-actinin (Pomiáes *et al*., 1999; Zhou *et al*., 1999; Kotaka *et al*., 2000). Mystique 3a, which has a PDZ domain and no LIM domain was located at the cytoskeleton (Figure 2A), which suggests that the PDZ domain mediates Mystique 2 targeting to the actin cytoskeleton. We tested this by expressing GFP-fused mutant Mystique 2 proteins in MCF-7 cells and visualizing polymerized actin with phalloidin by fluorescent micros-

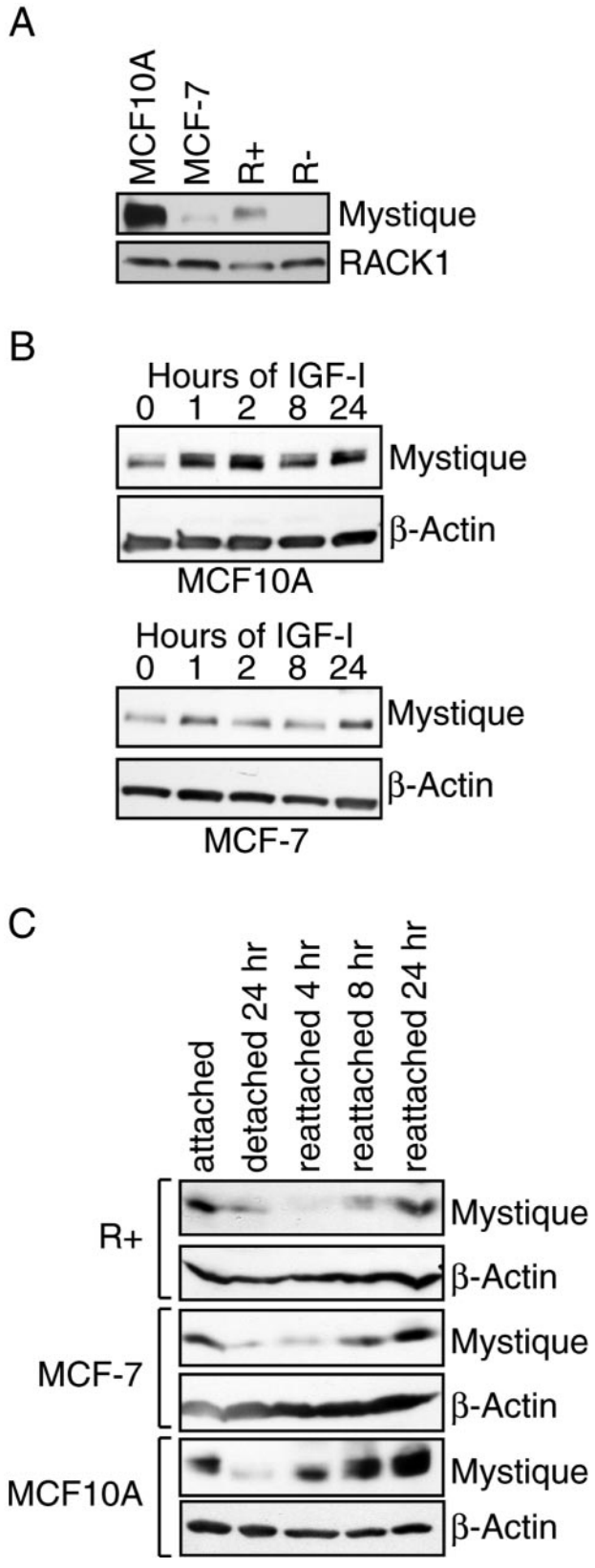

Figure 5. Mystique is highly expressed in MCF10A cells and is induced by IGF-I or ECM adhesion. (A) Cell lysates were prepared from MCF10A, MCF-7, and R+ and R− cells cultured in complete medium and assessed for Mystique 2 expression by using the anti-Mystique antiserum. Blots were reprobed with anti-RACK1 antibody as a loading control. (B) MCF10A or MCF-7 cells were starved from serum (24 h) before stimulation with IGF-I for the indicated times. Cell lysates were prepared for Western blotting with anti-Mystique antiserum or anti-β-actin as a loading control. (C) R+, MCF-7, or MCF10A cells were detached from tissues culture plates for 24 h before replating. At the indicated times, cell lysates were prepared for Western blotting with anti-Mystique antiserum and anti β-actin as a loading control.

copy. Figure 6C shows that both wild-type and LIM mutant (CC-SS) Mystique 2 were located at the actin cytoskeleton, whereas the PDZ (L80K) and double mutants displayed diffuse cytoplasmic staining. HA-tagged Mystique 2 mutants displayed similar localization patterns (our unpublished data). To test the requirement of the PDZ domain for association with α-actinin, HA-tagged mutant constructs, along with wild-type and empty vector control, were tested for coprecipitation with α-actinin by immunoprecipitation. Only those constructs that expressed an intact PDZ domain (wild-type and CC-SS) coprecipitated with α-actinin. (Figure 6D).

Together, these data indicate that Mystique 2 promotes cell attachment and this function is dependent on the PDZ domain but does not require an intact LIM domain. In addition, Mystique 2 cytoskeletal targeting and association with α-actinin require an intact PDZ domain. This suggests that the PDZ domain targets Mystique 2 to the actin cytoskeleton via α-actinin.

Silencing of Mystique 2 Expression Decreases Cell Adhesion and Migration in MCF-7 and MCF10A Cells

Mystique overexpression in MCF-7 cells suppressed clonogenic growth and enhanced the ability of cells to attach to ECM proteins. To test whether Mystique 2 is essential in MCF-7 cells or in MCF10A cells, which express it at high levels, we used siRNA to silence expression of Mystique protein and then assayed for cell attachment and migratory capacity.

Transfection of siRNA directed against *Mystique 2* into MCF-7 and MCF10A cells resulted in maximal silencing of protein expression 3 d posttransfection (Figure 7A). Reduced Mystique 2 expression was accompanied by a reduction in adhesion of ~30% to collagen and 60% to fibronectin, respectively, in MCF-7 and MCF10A cells, compared with cells transfected with a control siRNA (Figure 7B). Silencing of Mystique 2 expression in MCF-7 cells resulted in an ~50% decrease in migration of cells toward serum in Transwell plates (Figure 7C). This effect was even more pronounced in MCF10A cells, which displayed little motility when Mystique 2 was silenced.

Together, these results suggest that Mystique 2 is essential for both MCF-7 and MCF10A cells to mediate cell attachment and motility. The data also suggest that MCF10A cells may be more dependent on Mystique 2 for motility than MCF-7 cells.

DISCUSSION

This study describes the identification and characterization of a new IGF-I–responsive gene, *Mystique*, which is expressed as alternative splice variants in R+ and R− cells and encodes a protein with homology to a family of cytoskeletal-associated PDZ-LIM domain proteins. Our data indicate that Mystique can suppress anchorage-independent growth and

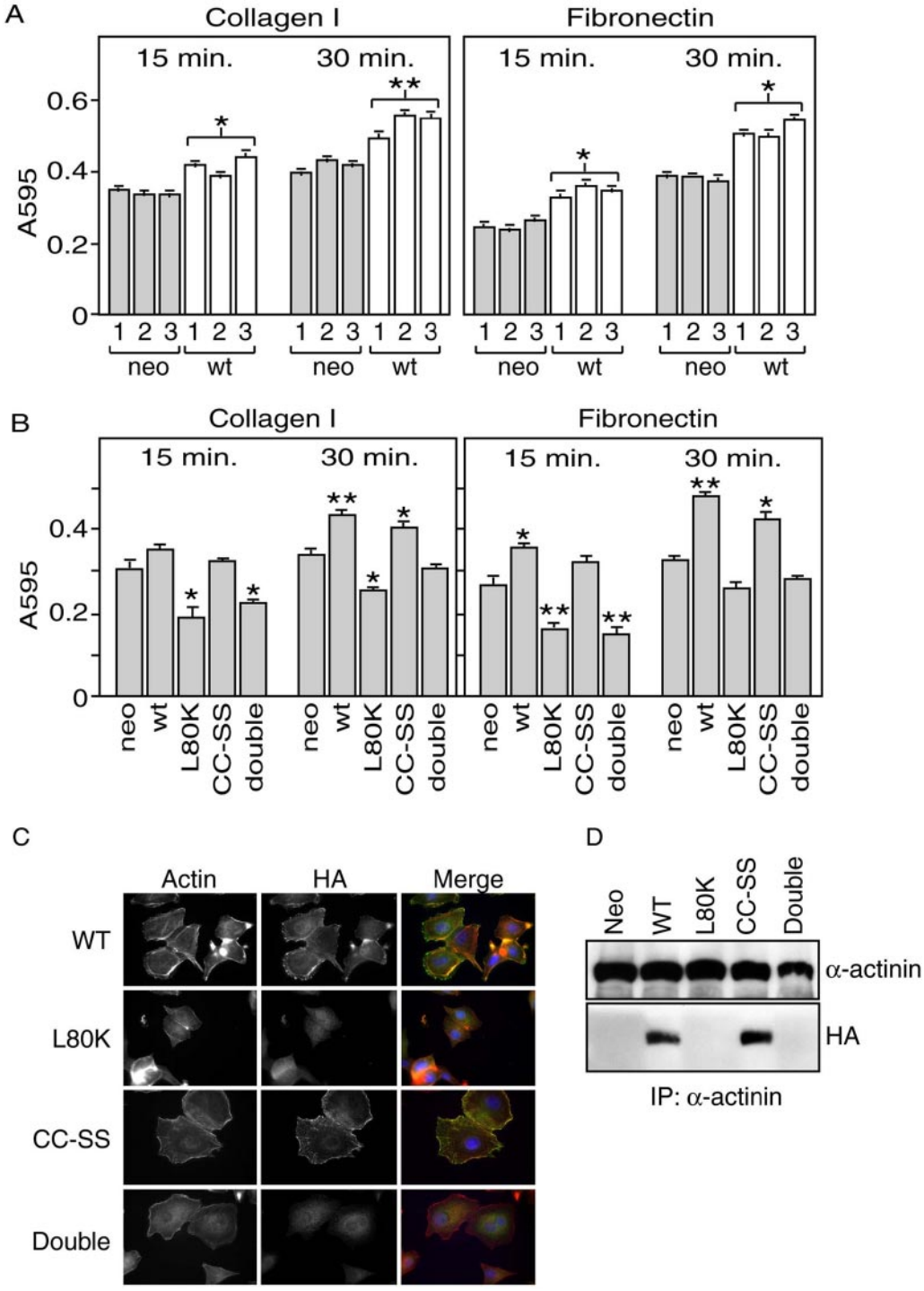

Figure 6. Overexpression of Mystique 2 enhances MCF-7 cell attachment, which requires an intact PDZ domain. (A) MCF-7 cell clones expressing Neo or WT Mystique 2 (WT) were allowed to adhere to either collagen (10 μg/ml) or fibronectin (5 μg/ml) for 15 or 30 min as indicated. Attached cells were stained with crystal violet, which was measured by absorbance at 595 nm. The mean absorbance from four wells was averaged for three clones of Neo and WT each, and then the means of each set of clones were compared with the means of Neo clones by using the Student's *t*-test. (B) Adhesion assays were carried out as in A with three clones each of MCF-7 cells expressing either Neo, WT, or Mystique-2 mutants. The means of each clone were compared with Neo by using Student's *t*-test (*$p < 0.01$, **$p < 0.001$). (C) GFP-fused Mystique 2 mutants were transiently transfected into MCF-7 cells, which also were incubated with TRITC-phalloidin to visualize the actin cytoskeleton. Cells were examined and photographed using fluorescence microscopy. (D) Cell lysates from MCF-7 cells transfected with either HA-tagged Mystique 2, or Mystique 2 mutants, or Neo control as indicated were immunoprecipitated with anti-α-actinin antibody and then analyzed by Western blotting with anti-HA or anti-α-actinin antibodies as indicated.

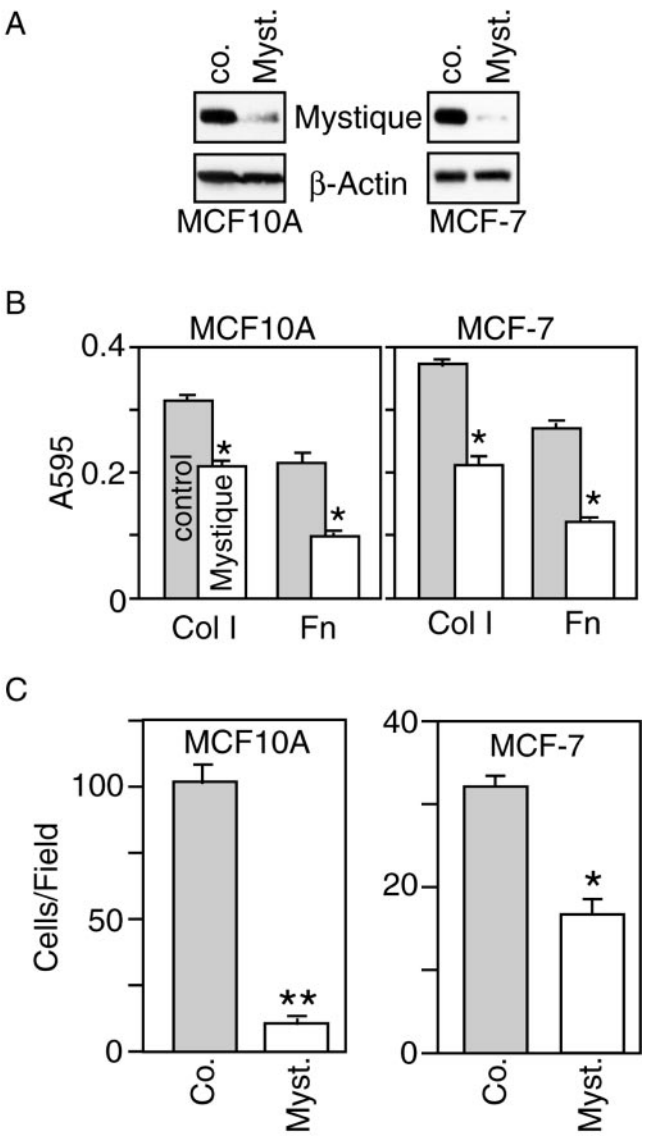

Figure 7. Silencing of Mystique disrupts cell attachment and suppresses motility. (A) MCF10A or MCF-7 cells were transfected with Mystique or control siRNA oligonucleotides and analyzed 3 d after transfection by Western blotting for expression of Mystique. After 60 h transfection with siRNA, MCF10A and MCF-7 cells were assayed for their ability to attach to either collagen or fibronectin (B) and to migrate toward complete media (C). For adhesion and motility assays, the means and standard deviations were calculated from quadruplicate (adhesion) or triplicate (motility) wells and compared using Student's *t*-test (*$p < 0.01$, **$p < 0.001$).

is necessary for cell attachment and migration in epithelial cells.

Mystique is the newest member of the ALP (Pomiáes *et al*., 1999), RIL (Kiess), and CLP-36 (Wang *et al*., 1995) subfamily of PDZ-LIM domain proteins. This subfamily is one of three related subfamilies of proteins, all of which contain a PDZ domain and one or more LIM domains. ALP, RIL, and CLP-36 each contain a single LIM domain, whereas the second subfamily, consisting of Enigma (Boden *et al*., 1998; Wu, 1994 #68), ENH (Kuroda *et al*., 1996), and ZASP/Cypher (Faulkner *et al*., 1999; Zhou *et al*., 1999), all have three LIM domains. The third subfamily is made up of two more distally related proteins, LIMK-1 (Mizuno *et al*., 1994) and LIMK-2 (Okano *et al*., 1995), each of which contains a kinase domain, two LIM domains, and a PDZ domain. These proteins are all thought to be involved in dynamic cytoskeletal-associated scaffolding activity, and it has been suggested that disturbances in LIM domain binding function is associated with developmental abnormalities and tumorigenesis (Cuppen *et al*., 1998; Bach, 2000).

Northern blot analysis indicated that *Mystique* variants are highly expressed in lung but are not expressed in muscle cells like many PDZ-LIM proteins. Analysis of a series of cell lines also showed expression of different splice variants with the *Mystique 3* transcript being more abundant than *Mystique 2* in R− cells, MRC-5 fibroblasts, and HeLa cells, whereas the *Mystique 2* transcript was more abundant in MCF-7, DU145, and Jurkat cells (our unpublished data). During the preparation of this article, a report on the rat homologue of Mystique (Pdlim2) gene was published (Torrado *et al*., 2004). This was identified in a cDNA library of transcripts expressed in rat corneal epithelial cells. Northern blot analysis showed high expression of the RNA in rat corneal epithelial cells but not other ocular tissues. Rat Pdlim2 also was expressed highly in the lung.

Mystique 2 was the only isoform detected in R+ cells or other cells. Neither Mystique 1 nor 3 was detected by Western blot analysis in any cell line tested so far, even in those cell lines where the *Mystique 3* RNA was more abundant than *Mystique 2*. RIL (Bashirova *et al*., 1998) and ZASP/Cypher (Hsia *et al*., 2003) also are predicted to be expressed as LIM-less isoforms, but their functions are not known.

Mystique 2 protein was expressed at much higher levels in the nontumorigenic breast epithelial cell line MCF10A than in R+ cells or in MCF-7 cells. Overexpression of Mystique 2 suppresses anchorage-independent growth of MCF-7 cells. This suggests that Mystique 2 may have tumor suppressor function. The *hMystique* gene is located on chromosome 8p21.2. Allelic loss of chromosome 8p21 occurs frequently in advanced ovarian and prostate cancers (Brown *et al*., 1999; Swalwell *et al*., 2002; Wolter *et al*., 2002). Other PDZ-LIM domain proteins have been associated with tumor suppressor function. RIL was identified as a gene product that is down-regulated in fibroblasts transformed by H-Ras (Kiess *et al*., 1995). TES (Tobias *et al*., 2001) and LIM kinase 1 (Higuchi *et al*., 1996) also have been shown to inhibit anchorage-independent growth. TES has been proposed as a tumor suppressor gene and is located in the fragile chromosome region (FRAG7) on human chromosome 7q31.1/2, which is frequently lost in tumors (Tobias *et al*., 2001). However, it is also possible that Mystique-mediated suppression of anchorage-independent growth occurs due to its other functions in promoting cell adhesion and migration. Overexpression of Mystique may cause cells to be highly dependent on attachment and thus decrease their ability to form colonies in soft agarose.

Our data indicate that the PDZ domain in Mystique is necessary to target the protein to the cytoskeleton and to associate with α-actinin. This is similar to observations with the rat orthologue (Torrado *et al*., 2004), with CLP-36, RIL, and with ALP (Faulkner *et al*., 1999; Pomiáes *et al*., 1999; Zhou *et al*., 1999; Kotaka *et al*., 2000). The colocalization of Mystique 2 with β1-integrins and α-actinin and lack of colocalization with paxillin or phosphotyrosine suggest that Mystique is located in fibrillar adhesions (Zamir *et al*., 2000). Fibrillar adhesions promote remodeling of the ECM and facilitate cell movement (Darribáere *et al*., 1990; Sechler and Schwarzbauer, 1997). These adhesions also are potentially involved in the migration of highly metastatic cancer cells

that have undergone epithelial mesenchymal transitions (Thiery, 2003).

Silencing of Mystique expression with siRNA had a dramatic effect on cell attachment and migration, especially in MCF10A cells. This suggests that Mystique is essential for migration of epithelial cells and may have a particular role in the migration of epithelial sheets. We observed that MCF10A cells migrate on ECM material as a sheet unlike MCF-7 cells and other transformed cells, which migrate as individual cells. Such a function for Mystique could be especially important in corneal epithelium, which expresses high levels of Mystique 2 in rat (Torrado *et al*., 2004), and migrates as a sheet during wound repair response to damage of the epithelial layer (Dalton and Steele, 2001).

Mutation of the PDZ domain alone was sufficient to abolish cell attachment by Mystique, suggesting that the LIM domain is not required for cell attachment. However, mutation of either the LIM or PDZ domains was sufficient to abolish suppression of anchorage-independent growth, suggesting that both domains are required for this function. LIM domains have been shown to interact with important signaling molecules, including receptors, kinases, and phosphatases. RIL has recently been shown to associate with synaptic α-amino-3-hydroxy-5-methyl-4-isoxazolepropionic acid (AMPA) glutamate receptors, where it is thought to regulate the trafficking and density of these receptors in synapses by targeting them to dendritic spines via association of the PDZ domain with the actin cytoskeleton (Schulz *et al*., 2004). The second and third LIM domains of Enigma can associate with the insulin receptor (Durick *et al*., 1996) and Ret/ptc2 (Durick *et al*., 1996, 1998), respectively. ENH (Kuroda *et al*., 1996) and ZASP/Cypher (Zhou *et al*., 1999) can associate with protein kinase C. The kinase Clik1 associates with the LIM domain of CLP-36 (Vallenius and Mèakelèa, 2002), and this causes relocalization of Clik1 from the nucleus to stress fibers, which may be important in regulating stress fiber formation (Vallenius and Mèakelèa, 2002). Identification of Mystique LIM domain interacting proteins also should shed light on its functions in regulating cell attachment migration and clonogenic growth.

In summary, Mystique is a PDZ-LIM domain adapter protein at the cytoskeleton whose expression is regulated by IGF-I and adhesion. Mystique enhances cell attachment and is essential for the migration of epithelial cells and also can suppress anchorage-independent growth. Future studies in primary epithelial tissues and tumors will determine the relative contributions of Mystique to normal epithelial cell or tumor cell migratory capacity.

ACKNOWLEDGMENTS

We are grateful to Kurt Tidmore for preparing the illustrations. This work was supported by grants from Enterprise Ireland, Tanaud Ireland, Inc., The Health Research Board, and Science Foundation Ireland.

REFERENCES

Adams, T. E., Epa, V. C., Garrett, T. P., and Ward, C. W. (2000). Structure and function of the type 1 insulin-like growth factor receptor. Cell Mol. Life Sci. *57*, 1050–1093.

Bach, I. (2000). The LIM domain: regulation by association. Mech. Dev. *91*, 5–17.

Baserga, R., Peruzzi, F., and Reiss, K. (2003). The IGF-1 receptor in cancer biology. Int. J. Cancer *107*, 873–877.

Bashirova, A. A., Markelov, M. L., Shlykova, T. V., Levshenkova, E. V., Alibaeva, R. A., and Frolova, E. I. (1998). The human RIL gene: mapping to human chromosome 5q31.1, genomic organization and alternative transcripts. Gene *210*, 239–245.

Boden, S. D., Liu, Y., Hair, G. A., Helms, J. A., Hu, D., Racine, M., Nanes, M. S., and Titus, L. (1998). LMP-1, a LIM-domain protein, mediates BMP-6 effects on bone formation. Endocrinology *139*, 5125–5134.

Brodt, P., Fallavollita, L., Khatib, A. M., Samani, A. A., and Zhang, D. (2001). Cooperative regulation of the invasive and metastatic phenotypes by different domains of the type I insulin-like growth factor receptor beta subunit. J. Biol. Chem. *276*, 33608–33615.

Brooks, P. C., Klemke, R. L., Schon, S., Lewis, J. M., Schwartz, M. A., and Cheresh, D. A. (1997). Insulin-like growth factor receptor cooperates with integrin alpha v beta 5 to promote tumor cell dissemination in vivo. J. Clin. Investig. *99*, 1390–1398.

Brown, M. R., Chuaqui, R., Vocke, C. D., Berchuck, A., Middleton, L. P., Emmert-Buck, M. R., and Kohn, E. C. (1999). Allelic loss on chromosome arm 8p: analysis of sporadic epithelial ovarian tumors. Gynecol. Oncol. *74*, 98–102.

Burgaud, J. L., and Baserga, R. (1996). Intracellular transactivation of the insulin-like growth factor I receptor by an EGF receptor. Exp. Cell Res. *223*, 412–419.

Casamassima, A., and Rozengurt, E. (1998). Insulin-like growth factor I stimulates tyrosine phosphorylation of p130(Cas), focal adhesion kinase, and paxillin. Role of phosphatidylinositol 3′-kinase and formation of a p130(Cas).Crk complex. J. Biol. Chem. *273*, 26149–26156.

Cuppen, E., Gerrits, H., Pepers, B., Wieringa, B., and Hendriks, W. (1998). PDZ motifs in PTP-BL and RIL bind to internal protein segments in the LIM domain protein RIL. Mol. Biol. Cell *9*, 671–683.

Dalton, B. A., and Steele, J. G. (2001). Migration mechanisms: corneal epithelial tissue and dissociated cells. Exp. Eye Res. *73*, 797–814.

Darribáere, T., Guida, K., Larjava, H., Johnson, K. E., Yamada, K. M., Thiery, J. P., and Boucaut, J. C. (1990). In vivo analyses of integrin beta 1 subunit function in fibronectin matrix assembly. J. Cell Biol. *110*, 1813–1823.

Doerr, M. E., and Jones, J. I. (1996). The roles of integrins and extracellular matrix proteins in the insulin-like growth factor I-stimulated chemotaxis of human breast cancer cells. J. Biol. Chem. *271*, 2443–2447.

Durick, K., Gill, G. N., and Taylor, S. S. (1998). Shc and Enigma are both required for mitogenic signaling by Ret/ptc2. Mol. Cell Biol. *18*, 2298–2308.

Durick, K., Wu, R. Y., Gill, G. N., and Taylor, S. S. (1996). Mitogenic signaling by Ret/ptc2 requires association with enigma via a LIM domain. J. Biol. Chem. *271*, 12691–12694.

Faulkner, G., *et al*. (1999). ZASP: a new Z-band alternatively spliced PDZ-motif protein. J. Cell Biol. *146*, 465–475.

Guvakova, M. A., Boettiger, D., and Adams, J. C. (2002). Induction of fascin spikes in breast cancer cells by activation of the insulin-like growth factor-I receptor. Int. J. Biochem. Cell Biol. *34*, 685–698.

Hermanto, U., Zong, C. S., Li, W., and Wang, L. H. (2002). RACK1, an insulin-like growth factor I (IGF-I) receptor-interacting protein, modulates IGF-I-dependent integrin signaling and promotes cell spreading and contact with extracellular matrix. Mol. Cell Biol. *22*, 2345–2365.

Higuchi, O., Baeg, G. H., Akiyama, T., and Mizuno, K. (1996). Suppression of fibroblast cell growth by overexpression of LIM-kinase 1. FEBS Lett. *396*, 81–86.

Hsia, D. A., *et al*. (2003). Differential regulation of cell motility and invasion by FAK. J. Cell Biol. *160*, 753–767.

Huang, C., Zhou, Q., Liang, P., Hollander, M. S., Sheikh, F., Li, X., Greaser, M., Shelton, G. D., Evans, S., and Chen, J. (2003). Characterization and in vivo functional analysis of splice variants of cypher. J. Biol. Chem. *278*, 7360–7365.

Jackson, J. G., Yoneda, T., Clark, G. M., and Yee, D. (2000). Elevated levels of p66 Shc are found in breast cancer cell lines and primary tumors with high metastatic potential. Clin. Cancer Res. *6*, 1135–1139.

Kiely, P. A., Sant, A., and O'Connor, R. (2002). RACK1 is an insulin-like growth factor 1 (IGF-1) receptor-interacting protein that can regulate IGF-1-mediated Akt activation and protection from cell death. J. Biol. Chem. *277*, 22581–22589.

Kiess, M., Scharm, B., Aguzzi, A., Hajnal, A., Klemenz, R., Schwarte-Waldhoff, I., and Schèafer, R. (1995). Expression of RIL, a novel LIM domain gene, is down-regulated in Hras-transformed cells and restored in phenotypic revertants. Oncogene *10*, 61–68.

Kim, B., and Feldman, E. L. (1998). Differential regulation of focal adhesion kinase and mitogen-activated protein kinase tyrosine phosphorylation during insulin-like growth factor-I-mediated cytoskeletal reorganization. J. Neurochem. *71*, 1333–1336.

Kim, B., van Golen, C. M., and Feldman, E. L. (2004). Insulin-like growth factor-I signaling in human neuroblastoma cells. Oncogene *23*, 130–141.

Kotaka, M., *et al*. (2000). Interaction of hCLIM1, an enigma family protein, with alpha-actinin 2. J. Cell. Biochem. *78*, 558–565.

Kuroda, S., Tokunaga, C., Kiyohara, Y., Higuchi, O., Konishi, H., Mizuno, K., Gill, G. N., and Kikkawa, U. (1996). Protein-protein interaction of zinc finger LIM domains with PKC. J. Biol. Chem. *271*, 31029–31032.

LeRoith, D., and Roberts, C. T., Jr. (2003). The insulin-like growth factor system and cancer. Cancer Lett. *195*, 127–137.

Lopez, T., and Hanahan, D. (2002). Elevated levels of IGF-1 receptor convey invasive and metastatic capability in a mouse model of pancreatic islet tumorigenesis. Cancer Cell *1*, 339–353.

Maloney, E. K., McLaughlin, J. L., Dagdigian, N. E., Garrett, L. M., Connors, K. M., Zhou, X. M., Blattler, W. A., Chittenden, T., and Singh, R. (2003). An anti-insulin-like growth factor I receptor antibody that is a potent inhibitor of cancer cell proliferation. Cancer Res. *63*, 5073–5083.

Manes, S., Mira, E., Gomez-Mouton, C., Zhao, Z. J., Lacalle, R. A., and Martinez, A. C. (1999). Concerted activity of tyrosine phosphatase SHP-2 and focal adhesion kinase in regulation of cell motility. Mol. Cell. Biol. *19*, 3125–3135.

Mauro, L., Bartucci, M., Morelli, C., Ando, S., and Surmacz, E. (2001). IGF-I receptor-induced cell-cell adhesion of MCF-7 breast cancer cells requires the expression of junction protein ZO-1. J. Biol. Chem. *276*, 39892–39897.

Mauro, L., Sisci, D., Bartucci, M., Salerno, M., Kim, J., Tam, T., Guvakova, M. A., Ando, S., and Surmacz, E. (1999). SHC-alpha5beta1 integrin interactions regulate breast cancer cell adhesion and motility. Exp. Cell Res. *252*, 439–448.

Michelsen, J. W., Schmeichel, K. L., Beckerle, M. C., and Winge, D. R. (1993). The LIM motif defines a specific zinc-binding protein domain. Proc. Natl. Acad. Sci. USA *90*, 4404–4408.

Miele, C., Rochford, J. J., Filippa, N., Giorgetti-Peraldi, S., and Van Obberghen, E. (2000). Insulin and insulin-like growth factor-I induce vascular endothelial growth factor mRNA expression via different signaling pathways. J. Biol. Chem. *275*, 21695–21702.

Mizuno, K., Okano, I., Ohashi, K., Nunoue, K., Kuma, K., Miyata, T., and Nakamura, T. (1994). Identification of a human cDNA encoding a novel protein kinase with two repeats of the LIM/double zinc finger motif. Oncogene *9*, 1605–1612.

Mulligan, C., Rochford, J., Denyer, G., Stephens, R., Yeo, G., Freeman, T., Siddle, K., and O'Rahilly, S. (2002). Microarray analysis of insulin and insulin-like growth factor-1 (IGF-1) receptor signaling reveals the selective up-regulation of the mitogen heparin-binding EGF-like growth factor by IGF-1. J. Biol. Chem. *277*, 42480–42487.

O'Connor, R., Kauffmann-Zeh, A., Liu, Y., Lehar, S., Evan, G. I., Baserga, R., and Blèattler, W. A. (1997). Identification of domains of the insulin-like growth factor I receptor that are required for protection from apoptosis. Mol. Cell. Biol. *17*, 427–435.

Okano, I., Hiraoka, J., Otera, H., Nunoue, K., Ohashi, K., Iwashita, S., Hirai, M., and Mizuno, K. (1995). Identification and characterization of a novel family of serine/threonine kinases containing two N-terminal LIM motifs. J. Biol. Chem. *270*, 31321–31330.

Pennisi, P. A., Barr, V., Nunez, N. P., Stannard, B., and Le Roith, D. (2002). Reduced expression of insulin-like growth factor I receptors in MCF-7 breast cancer cells leads to a more metastatic phenotype. Cancer Res. *62*, 6529–6537.

Playford, M. P., Bicknell, D., Bodmer, W. F., and Macaulay, V. M. (2000). Insulin-like growth factor 1 regulates the location, stability, and transcriptional activity of beta-catenin. Proc. Natl. Acad. Sci. USA *97*, 12103–12108.

Pomiáes, P., Macalma, T., and Beckerle, M. C. (1999). Purification and characterization of an alpha-actinin-binding PDZ-LIM protein that is up-regulated during muscle differentiation. J. Biol. Chem. *274*, 29242–29250.

Ponting, C. P., Phillips, C., Davies, K. E., and Blake, D. J. (1997). PDZ domains: targeting signalling molecules to sub-membranous sites. Bioessays *19*, 469–479.

Resnicoff, M. (1998). Antitumor effects elicited by antisense-mediated down-regulation of the insulin-like growth factor I receptor (review). Int. J. Mol. Med. *1*, 883–888.

Rottner, K., Krause, M., Gimona, M., Small, J. V., and Wehland, J. (2001). Zyxin is not colocalized with vasodilator-stimulated phosphoprotein (VASP) at lamellipodial tips and exhibits different dynamics to vinculin, paxillin, and VASP in focal adhesions. Mol. Biol. Cell *12*, 3103–3113.

Roudabush, F. L., Pierce, K. L., Maudsley, S., Khan, K. D., and Luttrell, L. M. (2000). Transactivation of the EGF receptor mediates IGF-1-stimulated shc phosphorylation and ERK1/2 activation in COS-7 cells. J. Biol. Chem. *275*, 22583–22589.

Schmeichel, K. L., and Beckerle, M. C. (1994). The LIM domain is a modular protein-binding interface. Cell *79*, 211–219.

Schulz, T. W., *et al*. (2004). Actin/alpha-actinin-dependent transport of AMPA receptors in dendritic spines: role of the PDZ-LIM protein RIL. J. Neurosci. *24*, 8584–8594.

Sechler, J. L., and Schwarzbauer, J. E. (1997). Coordinated regulation of fibronectin fibril assembly and actin stress fiber formation. Cell Adhes. Commun. *4*, 413–424.

Sell, C., Dumenil, G., Deveaud, C., Miura, M., Coppola, D., DeAngelis, T., Rubin, R., Efstratiadis, A., and Baserga, R. (1994). Effect of a null mutation of the insulin-like growth factor I receptor gene on growth and transformation of mouse embryo fibroblasts. Mol. Cell. Biol. *14*, 3604–3612.

Shieh, B. H., and Niemeyer, B. (1995). A novel protein encoded by the InaD gene regulates recovery of visual transduction in Drosophila. Neuron *14*, 201–210.

Swalwell, J. I., *et al*. (2002). Determination of a minimal deletion interval on chromosome band 8p21 in sporadic prostate cancer. Genes Chromosomes Cancer *33*, 201–205.

Thiery, J. P. (2003). Epithelial-mesenchymal transitions in development and pathologies. Curr. Opin. Cell Biol. *15*, 740–746.

Tobias, E. S., Hurlstone, A. F., MacKenzie, E., McFarlane, R., and Black, D. M. (2001). The TES gene at 7q31.1 is methylated in tumours and encodes a novel growth-suppressing LIM domain protein. Oncogene *20*, 2844–2853.

Torrado, M., Senatorov, V. V., Trivedi, R., Fariss, R. N., and Tomarev, S. I. (2004). Pdlim2, a novel PDZ-LIM domain protein, interacts with {alpha}-actinins and filamin A. Investig. Ophthalmol. Vis. Sci. *45*, 3955–3963.

Vallenius, T., and Mèakelèa, T. P. (2002). Clik *1*, a novel kinase targeted to actin stress fibers by the CLP-36 PDZ-LIM protein. J. Cell Sci. *115*, 2067–2073.

Wang, H., Harrison-Shostak, D. C., Lemasters, J. J., and Herman, B. (1995). Cloning of a rat cDNA encoding a novel LIM domain protein with high homology to rat RIL. Gene *165*, 267–271.

Wolter, H., Gottfried, H. W., and Mattfeldt, T. (2002). Genetic changes in stage pT2N0 prostate cancer studied by comparative genomic hybridization. BJU Int. *89*, 310–316.

Wu, R. Y., and Gill, G. N. (1994). LIM domain recognition of a tyrosine-containing tight turn. J. Biol. Chem. *269*, 25085–25090.

Zamir, E., *et al*. (2000). Dynamics and segregation of cell-matrix adhesions in cultured fibroblasts. Nat. Cell Biol. *2*, 191–196.

Zhang, D., and Brodt, P. (2003). Type 1 insulin-like growth factor regulates MT1-MMP synthesis and tumor invasion via PI 3-kinase/Akt signaling. Oncogene *22*, 974–982.

Zhang, D., Samani, A. A., and Brodt, P. (2003). The role of the IGF-I receptor in the regulation of matrix metalloproteinases, tumor invasion and metastasis. Horm. Metab. Res. *35*, 802–808.

Zhou, Q., Ruiz-Lozano, P., Martone, M. E., and Chen, J. (1999). Cypher, a striated muscle-restricted PDZ and LIM domain-containing protein, binds to alpha-actinin-2 and PKC. J. Biol. Chem. *274*, 19807–19813.